NJC

Accepted Manuscript

This is an *Accepted Manuscript*, which has been through the Royal Society of Chemistry peer review process and has been accepted for publication.

Accepted Manuscripts are published online shortly after acceptance, before technical editing, formatting and proof reading. Using this free service, authors can make their results available to the community, in citable form, before we publish the edited article. We will replace this *Accepted Manuscript* with the edited and formatted *Advance Article* as soon as it is available.

You can find more information about *Accepted Manuscripts* in the Information for Authors.

Please note that technical editing may introduce minor changes to the text and/or graphics, which may alter content. The journal's standard Terms & Conditions and the Ethical guidelines still apply. In no event shall the Royal Society of Chemistry be held responsible for any errors or omissions in this *Accepted Manuscript* or any consequences arising from the use of any information it contains.

ROYAL SOCIETY OF CHEMISTRY

www.rsc.org/njc

New Journal of Chemistry RSCPublishing

ARTICLE

Facile synthesis of monolithic mayenite with well-defined macropores via an epoxide-mediated sol-gel process accompanied by phase separation†

Cite this: DOI: 10.1039/xoxxoooooox

Received ooth January 2012,
Accepted ooth January 2012

DOI: 10.1039/xoxxoooooox

www.rsc.org/

Xingzhong Guo[a], Xiaobo Cai[a], Jie Song[a], Yang Zhu[b], Kazuki Nakanishi[b], Kazuyoshi Kanamori[b], Hui Yang[a]*

Monolithic mayenite with well-defined macropores has been successfully synthesized from ionic precursors via a sol-gel process accompanied by phase separation. The addition of propylene oxide (PO) to the starting solution leads to homogenous gelation and modifies the gel skeleton, whereas the addition of poly(ethylene oxide) (PEO) induces the phase separation. Glycol acts as a chelating agent to suppress the precipitation of Ca^{2+} ions, and formamide works as a drying control chemical additive to enhance the drying behavior. Appropriate amount of solvents, PEO, and PO allows the formation of calcium aluminate gels with co-continuous macroporous structure. The reaction mechanism of sol-gel process of Ca-Al-O system is also investigated by TG-DSC, FT-IR and NMR. The dried gels are amorphous and crystalline phase $Ca_{12}Al_{14}O_{32}Cl_2$ forms after heat-treatment at 1000 ℃ in air, while the macroporous structure is preserved. The resultant monoliths before and after heat-treatment both possess high porosity and smooth and dense skeletons.

1 Introduction

Mayenite ($12CaO \cdot 7Al_2O_3$, C12A7) in $CaO\text{-}Al_2O_3$ binary system is a promising functional ceramics duo to its special nanoporous structure. The crystal structure of C12A7 is cubic with a lattice constant of 1.199 nm. Stoichiometric formula for one unit cell (Z=2) of 118 atoms is $[Ca_{24}Al_{28}O_{64}]^{4+} \cdot 2O^{2-}$, the former part denotes the positively charged framework containing 12 crystallographic "cages", while two extra O^{2-} ions occupy two out of 12 Ca-Al-O cages, referred to as "free oxygen ions".[1-3] Although the crystal is a stable ceramic, many studies have demonstrated that these free oxygen ions can be replaced by other anions with similar ionic radii to the cage size such as Cl^-, OH^-, O^-, H^- ions,[4-8] or electrons.[9-11] When free oxygen ions are replaced with electrons, C12A7 is known as a novel room-temperature-stable electride[8-16] with low work function, and exhibits properties for application in electronic devices, electrochemistry, and other areas.[17,18]

Up to now, C12A7 powders, single crystals, and films have been synthesized by numerous techniques. For example, solid phase reaction[19] and sol-gel process[20] for powders, Czochralski growth[8,21] for single crystals, sol-gel process[22] and pulsed laser deposition (PLD)[9,23] for films. However, porous mayenite materials with controlled macropores and co-continuous structure have not been reported yet. Also, there are no studies on the fabrication of macroporous mayenite monoliths by sol-gel process accompanied by phase separation. Since porous materials have attracted more and more attention,[24-26] synthesis of porous C12A7 seems to be a new research direction of this material.

The sol-gel process accompanied by phase separation has been developed to be a new wet chemistry method for preparation of porous monoliths. A sol-gel reaction progresses parallel to the phase separation, freezing the phase-separating transient structures, which results in the "co-continuous" structure in the micrometer scale.[27-29] First reported by Gash et al.,[30] epoxide-mediated sol-gel reaction using aqueous solution of metal salts has been used to prepare monolithic gels of metal hydroxides or oxyhydroxides in a wide variety of metals. In a partially hydrolyzed solution of metal salts, epoxide acts as a proton scavenger to raise the solution pH moderately and uniformly, which leads to the hydrolysis and uniform condensation of aquo-cations.[31-33]

Recently, combining the polymerization-induced phase separation with epoxide-mediated sol-gel technique, more new porous monoliths have been prepared, such as alumina,[34] zirconia,[35] iron(III) oxides,[36] methylsilsesquioxane,[37,38] and mixed oxides, $LiFePO_4$/Carbon,[39] $AlPO_4$,[40] mullite,[41] and cordierite.[42] Compared to alumina or mullite system, however, it is not easy to obtain calcium aluminate monolithic gels since high concentration of Ca^{2+} ions tends to form precipitation during gelation in the present of polymers.[43] In addition, the gels inevitably shrink after evaporation drying.

In this study, we report a facile synthetic route for formation of monolithic mayenite with well-defined macropores from calcium chloride dehydrate and aluminum chloride hexahydrate. Poly(ethylene oxide) acts as a phase separation inducer, and propylene oxide acts as a gelation agent. In order to obtain the porous monoliths, we have also used two additives: glycol is used as a chelating agent to suppress the precipitation of Ca^{2+} ions, and formamide is added as a drying control chemical additive to enhance the drying behavior of the gels. The effect of the starting compositions on the gel morphologies and the reaction mechanism of the sol-gel process are investigated. In addition, the influence of heat-treatment condition on the crystalline phase and macroporous structure is also discussed. With further reduction treatment, this porous mayenite material has potential applications in catalysis, separation and electrodes.

2 Experimental

2.1 Materials

Calcium chloride dihydrate ($CaCl_2$ $2H_2O$: Sigma–Aldrich Co., USA, 99+%) was utilized as a calcium source, and aluminum chloride hexahydrate ($AlCl_3$ $6H_2O$: Sigma–Aldrich Co., USA, 99%) as an aluminum source. Mixture of distill water and ethanol (C_2H_6O: Sinopharm Chemical Reagent Co., Ltd, China, AR) was used as a solvent. Poly (ethylene oxide) (PEO: Aladdin Co., China, AR) with average molecular weight, M_w, of 300,000 was used as a phase separation inducer. Propylene oxide (PO: Sigma–Aldrich Co., USA, 99.5%) was added as a gelation agent. Glycol and Formamide (EG and FA: Sinopharm Chemical Reagent Co., Ltd, China, AR) was added as a chelating agent and drying control chemical additive, respectively. All reagents were used as received.

Table 1 Starting compositions of the reaction mixtures in this study.

Materials[a]	H_2O (mL)	EtOH (mL)	PO (mL)	PEO (g)
CA1	3.00	3.00	1.50	0
CA2	3.00	3.00	1.50	0.040
CA3	3.00	3.00	1.50	0.080
CA4	3.00	3.00	1.50	0.100
CA5	3.00	3.00	1.50	0.160
CA6	3.00	3.00	1.40	0.080
CA7	3.00	3.00	1.70	0.080
CA8	3.00	3.00	1.90	0.080
CA9	3.20	2.50	1.50	0.080
CA10	3.20	2.50	1.70	0.080
CA11	3.20	2.50	1.90	0.080

[a] 1.044 g $CaCl_2$ $2H_2O$, 2.000g $AlCl_3$ $6H_2O$, 0.40 mL EG and 0.50 mL FA were used the same in each reaction mixture.

2.2 Synthesis

The starting compositions were listed in Table 1. In a typical synthesis, 1.044 g of $CaCl_2$ $2H_2O$ and 2.000g of $AlCl_3$ $6H_2O$ were dissolved in a mixture of 3.00 ml distilled water and 3.00 ml ethanol. Then, 0.40 ml EG (EG / Ca(II) = 1 in molar ratio), W_{PEO} g of PEO, and 0.50ml FA were added in sequence. After stirring at room temperature for 1 h, the resultant transparent solution was cooled to 0 ℃ in an ice/water bath and V_{PO} ml of PO was added slowly (about 1 mL min^{-1}) with vigorous stirring. After mixing for 2 min, the obtained homogeneous solution was degassed by ultrasonication for 15 s in order to remove bubbles, followed by gelation at 40 ℃. After gelation, the obtained wet gels were aged at 40 ℃ for 24 h and then evaporation-dried at 60 ℃ for 72 h. Some of the resultant xerogels were subsequently heat-treated at various temperatures up to 1100 ℃ for 2 h with a heating rate of 5 ℃ min^{-1}.

2.3 Characterization

Morphologies of dried gels and heat-treated gels were observed by a field-emission scanning electron microscope (FESEM: SIRION-100, FEI Co., Holland). Thermogravimetric-differential scanning calorimetry (TG-DSC: SDT-Q600, TA Instrument, USA) to 1100 ℃ was performed on the sample at a heating rate of 5 ℃ min^{-1} while continuously supplying air at a rate of 100 mL min^{-1}. Chemical bonding information on the dried gels was investigated with Fourier transform infrared spectroscopy (FT-IR: Nicolet 5700, ThermoFisher Co., USA). ^{27}Al nuclear magnetic resonance (NMR: DD2-600, Agilent, USA) was performed on aluminum solutions at ambient temperature using one nmr sample probe. The chemical shift reference was an aqueous solution of 1mol L^{-1} $AlCl_3$, assigned a chemical shift of 0 ppm. The crystal structure was confirmed by powder X-ray diffraction (XRD: Empyrean 200895, PANalytical B.V., Holland). Macropore size distributions over the diameter from 20 nm to 100 μm were evaluated by mercury porosimetry (AutoPore IV 9510, Micromeritics Instruments, USA). Meso- and micropores were characterized by N_2 adsorption−desorption isotherms (Autosorb-1-C, Quantachrome Instruments, USA) and the samples were first degassed at 100 ℃ under vacuum. The pore size distribution and the surface area were calculated by the Barrett-Joyner-Halenda (BJH) method and Brunauer-Emmett-Teller (BET) method, respectively. The porosity (%) of each sample was calculated as $[(1 - \rho_b)/\rho_s] \times 100$, where ρ_b and ρ_s refers to the bulk and skeletal densities, respectively.

3 Results and discussion

3.1 Preparation of Monolithic Gels by Sol-Gel Process

In this study, we utilized a low-cost and efficient sol-gel method from ionic precursors, polymer, and epoxide to obtain calcium aluminate xerogels. The starting solutions with the compositions listed in Table 1 were homogeneous and transparent. The addition of PO quickly formed gels (about 18 min in CA3), while gelation was not observed without PO. However, the gel was heterogeneous in the absence of EG due to the precipitation of Ca^{2+} ions during the sol-gel process. Diols, used as chelating agents by coordinating to metal ions,[44] are able to develop bonds with Ca^{2+} ions to suppress the precipitation. In the present system, EG is used as a chelating agent. In some cases, diols or polyols are good solvents for the preparation of porous monoliths.[36,45] Samples using EG as one of the solvent were prepared by substituting ethanol with

equivalent volume of EG. However, translucent gels were obtained after long gelation time of 12 h. Thus, 0.40 ml EG (EG / Ca(II) = 1 in molar ratio) was added in each sample.

For the purpose of keeping the stoichiometry, the resultant wet gels were dried at 60 ℃ after aging without washing. Crack-free dried gels could be obtained when the gels were dried in a closed container with a pinhole. However, obvious shrinkage of gels was inevitable without FA. In sol-gel process of preparation of aerogels, drying control chemical additives (DCCAs) are often used to control the pore sizes and enhance the drying behavior of the gel network, and FA is the most commonly used.[46,47] We employ this DCCA in this study. Since FA is also a gelation agent for preparation of some porous monoliths[27,48-50], we first confirmed in a separate experiment that, gelation was not observed when using an equivalent mole of FA to that of PO (CA3). This indicates that FA does not act as a gelation agent in the present system. Fig. 1 shows dried gels prepared with varied V_{FA}. Almost no macropores are obtained after drying when no FA is added (Fig. 1a); whereas the addition of an appropriate amount of V_{FA} produces a homogeneous co-continous macropores (Fig. 1b); with further increased V_{FA}, the macropores become smaller again (Fig. 1c). Extra FA increases the volume of solution and destabilizes the whole system, which causes collapse of network after drying.

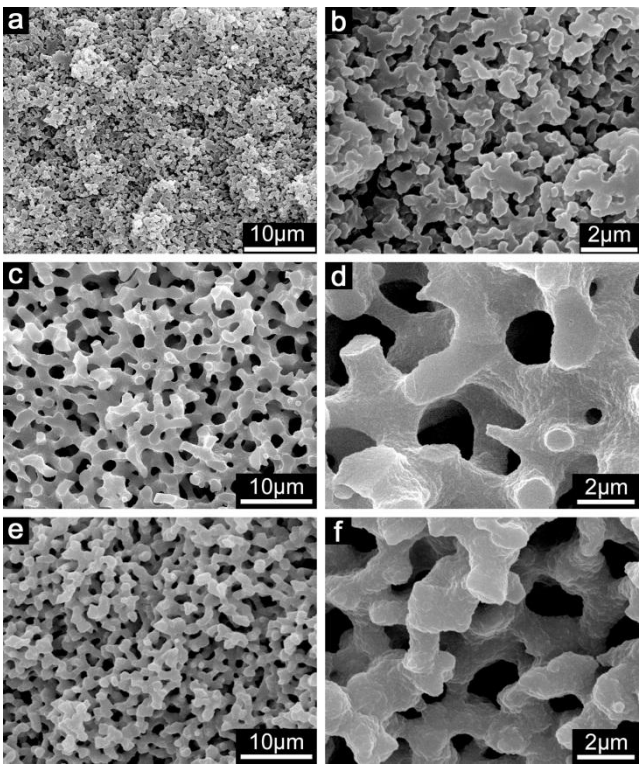

Fig. 1 SEM images of dried gels prepared with varied V_{FA} at different magnifications: (a) and (b) 0, (c) and (d) 0.5 ml (CA3), (e) and (f) 1.0 ml.

Fig. 2a shows appearance of a dried gel, and Fig. 2b-f shows SEM images of dried gels prepared with varied W_{PEO}. In the absence of PEO, almost no phase separation takes place and gel with no macropores is obtained (Fig. 2b). On the other hand, with increased W_{PEO}, morphologies vary remarkably as macroporous structure becomes coarsened. In CA2, only isolated pores of about 0.5 μm is observed (Fig. 2c), whereas the addition of an appropriate W_{PEO} forms a homogeneous co-continuous gel skeleton with smooth skeleton surfaces (CA3, Fig. 2d). Further increase in W_{PEO} leads to a coarsened co-continuous structure (CA4, Fig. 2e) and then a gel matrix with particle aggregates (CA5, Fig. 2f). In the case of the sol-gel method accompanied by phase separation, the morphologies in submicrometer-to-micrometer scale of the gels are formed by fixing the transient morphologies formed during the phase separation.[27] The increase in pore size is a result of the higher phase-separation tendency between the gel and liquid phases.

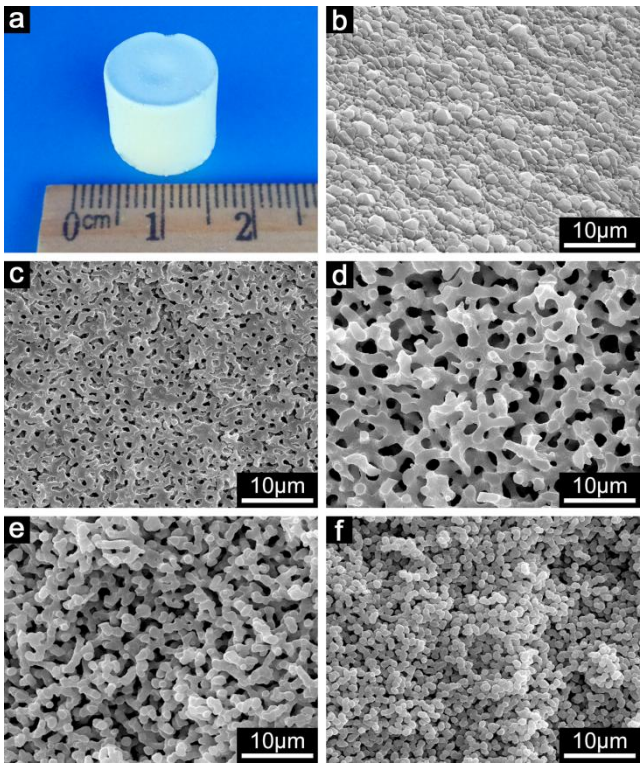

Fig. 2 (a) Appearance of a dried gel and SEM images of dried gels prepared with varied W_{PEO}: (b) CA1, (c) CA2, (d) CA3, (e) CA4, (f) CA5.

To clarify the role of PEO, thermal analysis and chemical bonding analysis were carried out to determine the distribution of PEO between gel phase and liquid phase. TG-DSC curves for gels prepared without PEO (CA1) and with PEO (CA3) are depicted in Fig. 3a. It shows that TG-DSC curves for gels with and without PEO are similar. The evaporation of remaining water and organic solvent takes place below 200 ℃. The weight loss between 200 ℃ and 300 ℃ and exothermic peak at around 300 ℃ are attributed to the dehydration of calcium chloride and decomposition of organic species, such as chlorohydrin, generated by the ring-opening reaction of PO; however, no exothermic peak for the combustion of PEO is found.[34] The weight loss between 300 ℃ and 400 ℃ and endothermic peak at around 400 ℃ is ascribed to

transformation of amorphous aluminum hydroxide to γ-Al_2O_3. No obvious weight loss is observed above 500 ℃.

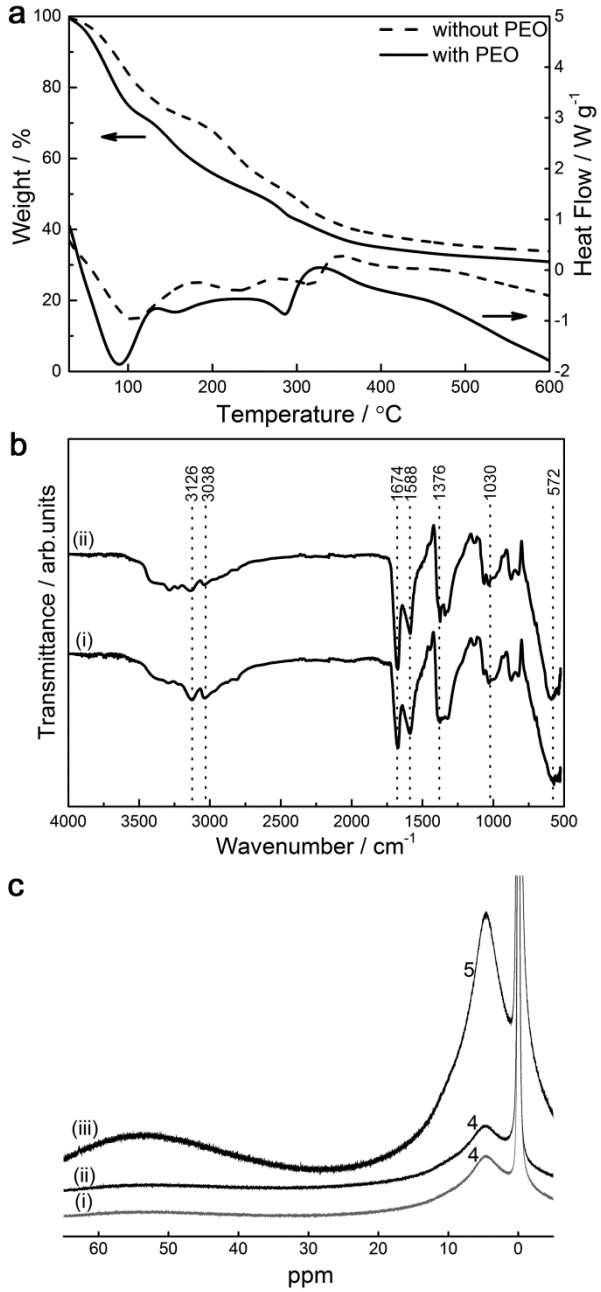

Fig. 3 (a) TG-DSC curves of dried gels prepared without PEO (CA1, dash line) and with PEO (CA3, solid line) under an air atmosphere. (b) FT-IR spectra of dried gels prepared without PEO (CA1, i) and with PEO (CA3, ii). (c) ^{27}Al-NMR spectra of $AlCl_3$ solutions without PEO (i) and with PEO (ii, iii). The pH values adjusted by varied V_{PO} are indicated.

Fourier transform infrared spectra of CA1 (i) and CA3 (ii) are shown in Fig. 3b. It shows no obvious differences between two spectra. Information about the main bands are as follow: stretching vibration of Al−O bonds (572 cm^{-1}), stretching vibration of C−C bonds (1,030 cm^{-1}), stretching vibration of C−N bonds (1,376 cm^{-1}), bending vibration of N−H bonds (1,588 cm^{-1}), stretching vibration of C=O groups (1,674 cm^{-1}), stretching vibration of H−O bonds (3,038 cm^{-1}) and stretching vibration of N−H bonds (3,126 cm^{-1}). The results of these data reveal that FA and EG is distributed to the gel phase. It also indicates that there is strong hydrogen-bond interaction between amide groups and hydroxyl groups as stretching vibration peaks of N-H and O-H bonds shift to small wavenumber area. However, no characteristic peaks for PEO are found.[41] This indicates that PEO is preferentially distributed into the liquid phase composed mainly of solvent mixtures, similarly to the case of Al_2O_3 monoliths[34] and monolithic $LiFePO_4$/Carbon composites.[39]

Also, NMR analysis was carried out to investigate the interaction between PEO and aluminum oligomers. ^{27}Al-NMR spectra of $AlCl_3$ solutions without PEO (i) and with PEO (ii, iii) are shown in Fig. 3c, and the pH values adjusted by varied V_{PO} are indicated. Each spectrum consists of two resonances: a sharp line at 0 ppm corresponding to $[Al(H_2O)_6]^{3+}$, and a broad line centered at 5ppm corresponding to polymerized aluminum aqua ions. Resonance at 5ppm increases with an increased pH value, indicating the process of condensation. It is expected to observe new chemical shift at high ppm area when Al^{3+} is coordinated by alkylene oxide segments, such as (-CH_2-CH_2-O-) units in PEO.[51,52] Yet no chemical shift is observed after the addition of PEO (from solution i to solution ii) and the increase in pH value (from solution ii to solution iii). This implies the hydrolyzates, Al-OH species, interact with EO units through hydrogen-bonds like Si-OH species in SiO_2 system.[27] However, considering the acidity of Al-OH, this hydrogen-bond interaction is relatively weak and is easy to be broken. The sol-gel process accompanied by phase separation of Ca-Al-O system in the present compositions can be described as follow (Fig. 4).

Aquo-aluminum ions have relatively weak hydrolysis equilibrium in the solution. After the addition of PO, further hydrolysis reaction takes place duo to the irreversible ring-opening reaction of PO, and aluminum oligomers are formed through olation. PEO chain forms hydrogen-bond with aluminum oligomers, leading to the polycondensation of aluminum oligomers. On the other hand, Ca^{2+} ions chelated by EG are absorbed on Al-O-Al polymer chain, and to some extent, reduce the compatibility between polymerizing aluminum oligomers and PEO chain because of steric effect. In addition, Amide groups in FA have hydrogen-bond interaction with surface hydroxyl groups of Al-O-Al polymer chain, suppressing the polycondensation of alumina oligomers and controlling the final uniform degree of polymerization. Further increase in the degree of polymerization causes the reduction of compatibility between polymerizing aluminum oligomers and PEO chain, which leads to the phase separation and the formation of PEO-rich liquid phase and calcium aluminate-rich gel phase. This transient morphology is then frozen by the parallel sol-gel transition.

The macropore size distributions of dried gels prepared with varied W_{PEO} are shown in Fig. 5. Mercury porosimetry analysis indicates that the gels possess narrow pore size distribution, and median macropore sizes of CA3 and CA4 are 1.8 and 1.2 μm,

respectively. The porosities calculated from the bulk density and skeletal density are 59.6 % and 54.5 % for CA3 and CA4, respectively. As PEO is a phase separation inducer, phase separation tendency becomes higher when W_{PEO} increases, and forms larger macropores but relatively weak skeleton. This structure undergoes to shrink after drying, which results in the decrease of pore size and pore volume.

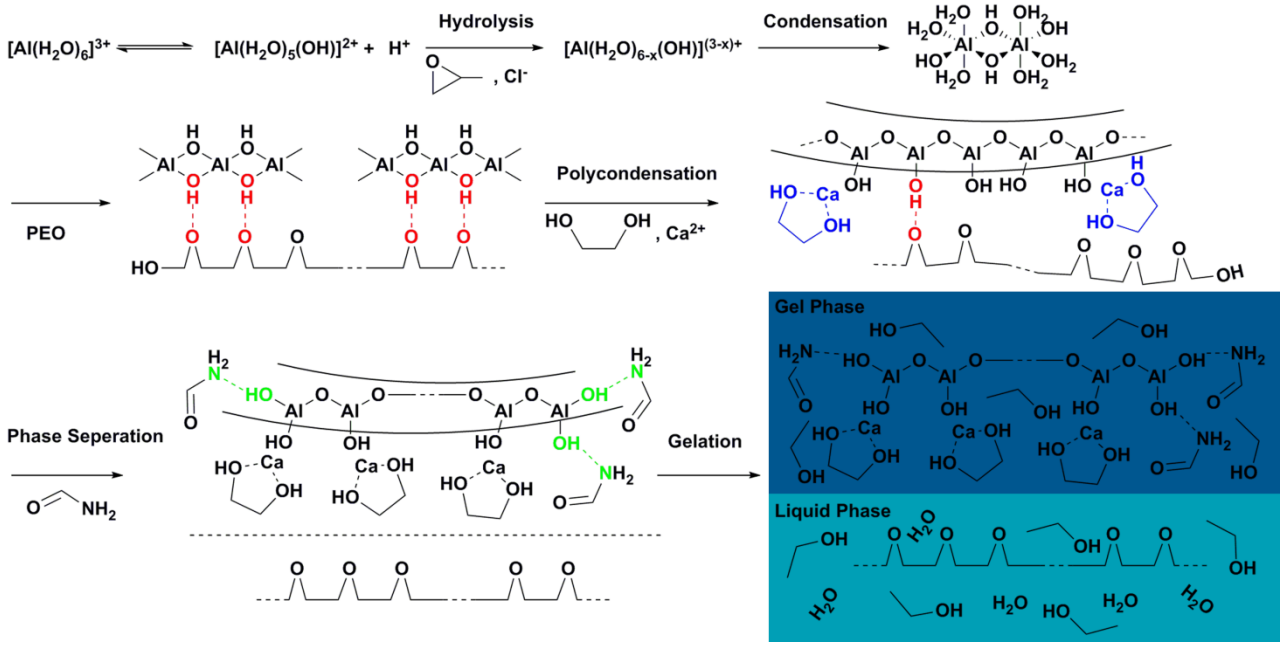

Fig. 4 The sol-gel process accompanied by phase separation of Ca-Al-O system.

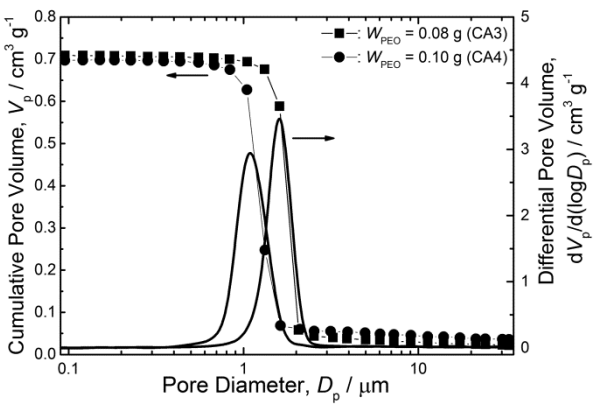

Fig. 5 Macropore size distributions of dried gels CA3 and CA4.

In the present system, the increasing rate of pH is one of the most important factors. As mentioned above, gelation of metal salts solution can be induced by using epoxides as gelation agents. Epoxides act as proton scavengers by irreversible ring-opening reaction and cause the solution pH increasing moderately and uniformly throughout the solution.[29] Nakanishi et al. have investigated several kinds of epoxides, such as PO, trimethylene oxide (TMO), and 1,2-epoxybutane (EB), and PO is considered to be a better choice for the preparation of porous monoliths.[36,43] Here, we chose PO as a proton scavenger and investigate the effect of PO on the gel morphology.

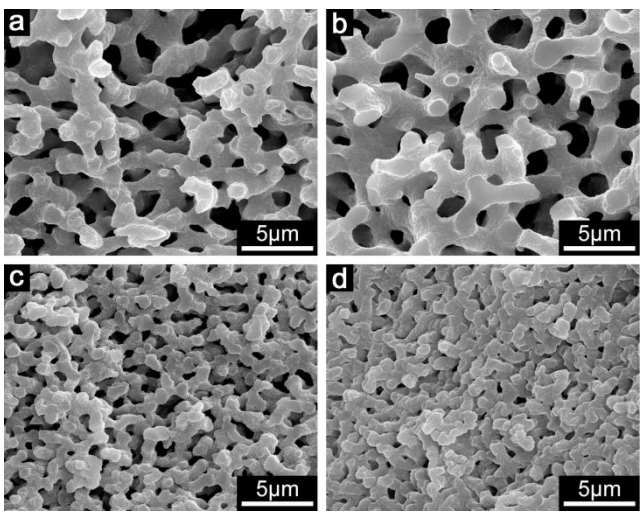

Fig. 6 SEM images of dried gels prepared with varied V_{PO}: (a) CA6, (b) CA3, (c) CA7, (d) CA8.

The pH value increased dramatically from 3 to 5 in a few minutes after the addition of PO, and then increased gradually with time, reaching 6 before gelation. The increase in V_{PO} effectively shortens the gelation time from 30 min to 8 min. The effect of varied V_{PO} on the gel morphology is shown in Fig. 6. The macroporous structure becomes smaller with an increase in V_{PO} and almost no macropores can be observed when 1.8ml PO is added (CA8, Fig. 6d). Because PO accelerates the increase of pH value, the timing of the sol-gel transition parallel

to the phase separation is in advance when V_{PO} increases. As a result, transient structure with small domain size in the early phase-separating stage is fixed. Even when V_{PO} increases slightly, the change is remarkable (From Fig. 6b to 6c). It is also interesting that, in a high ratio of water to ethanol system, further increase in V_{PO} brings about similar change on morphology as above, as shown in Fig. 7. However, the skeleton is not smooth with many small particles on it (Fig. 7d). PO influences both macropores and the gel skeletons. The choice of appropriate amount of PO allows the formation of gels with controlled smooth co-countious structure.

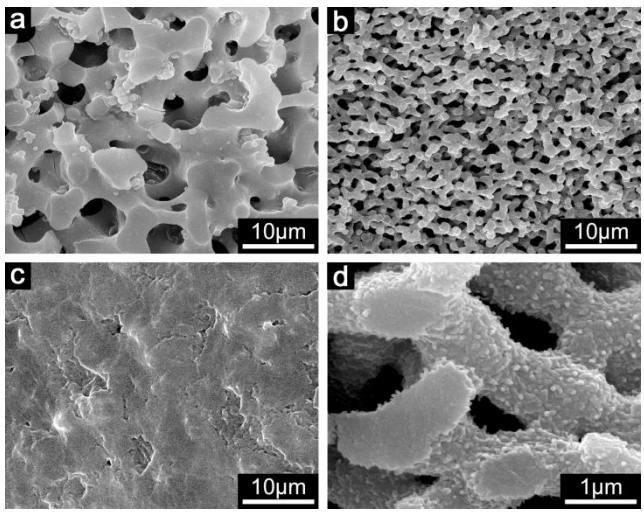

Fig. 7 SEM images of dried gels prepared with high ratio of water to ethanol and varied V_{PO}: (a) CA9, (b) CA10, (c) CA11, (d) CA10, at larger magnification.

3.2 Heat-treatment and Crystallization

The heat-measurement was performed on the sample CA3. Variation of XRD patterns with heat-treatment temperature in air is depicted in Fig. 8. No specific peaks attributed to as-dried gel and the samples heat-treated below 300 ℃ are observed, indicating the amorphous phase. While the weak diffraction patterns between 400 ℃ and 700 ℃ are ascribed to γ-Al_2O_3 and CaO. The process of crystallization initiates at 900 ℃ and completes at 1000 ℃. The obtained heat-treated samples are not $Ca_{12}Al_{14}O_{33}$ but $Ca_{12}Al_{14}O_{32}Cl_2$ (PDF#45-0568).[53,54] The extra O^{2-} ions in mayenite's nanoporous structure are replaced by Cl^- ions duo to chloride precursors and heat-treatment in air in this study. The existence of chlorine is also confirmed by EDS analysis (not shown). Chlorine can be removed by sintering these samples in O_2 atmosphere. However, this step is not necessary for applications such as electrical devices since further reduction treatment is needed. In addition, the complete crystallization temperature of $Ca_{12}Al_{14}O_{32}Cl_2$ is about 100 ℃ lower than that of pure C12A7.[19,21]

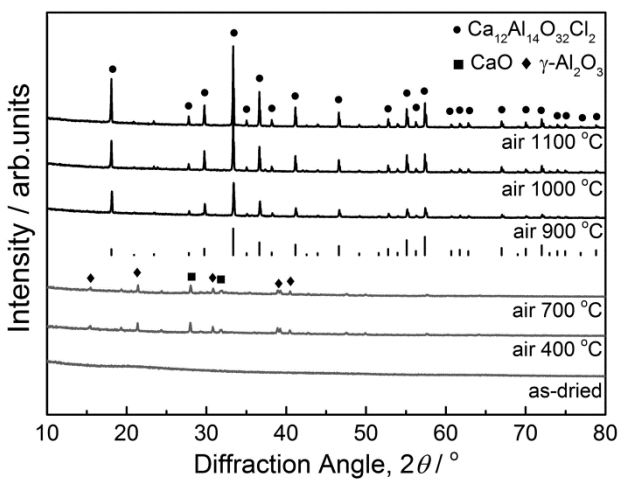

Fig. 8 XRD patterns of sample CA3 as-dried and heat-treated at different temperatures in air.

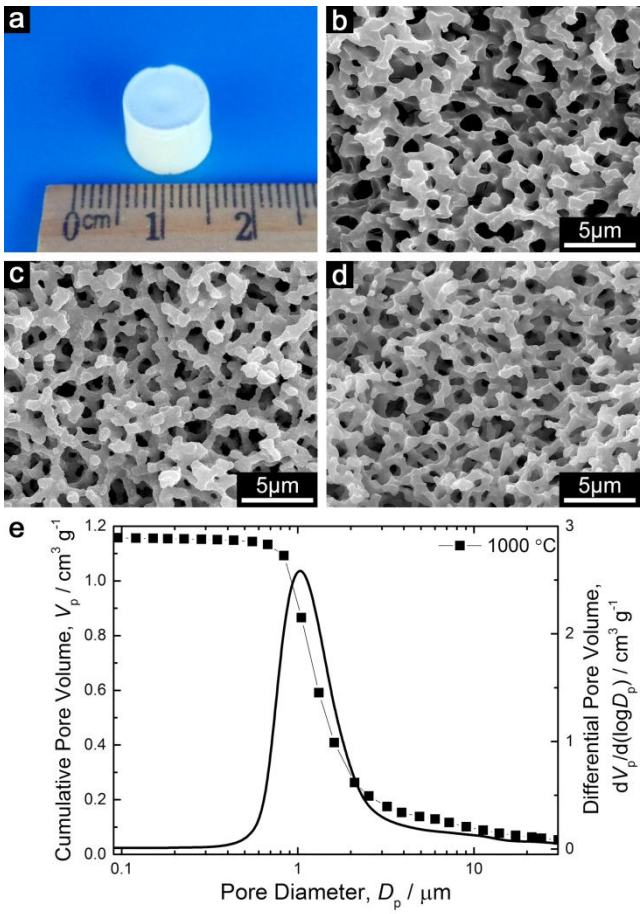

Fig. 9 (a) Appearance of sample CA3 after heat-treatment and SEM images of samples heat-treated in air at different temperature: (b) 400 °C, (c) 700 °C, (d) 900 °C, (e) 1000 °C, (f) 1100 °C. (g) Macropore size distribution of CA3 heat-treated at 1000 °C.

The appearance of CA3 heat-treated at 1000 ℃ and the macroporous morphologies of heat-treated samples are shown in Fig. 9. White crack-free monolith with volume shrinkage of about 50 % can be obtained after careful heat-treatment in air (Fig. 9a). The macroporous structure is preserved after heat-treatment at different temperatures. Below the crystallization temperature of $Ca_{12}Al_{14}O_{32}Cl_2$, macroporous structure of heat-treated samples change slightly (Fig. 9b); above the crystallization temperature, the skeleton becomes finer but

retains smooth surface (Fig. 9c); further increase in heat-treatment temperature causes the collapse of interconnected macropores in some regions (Fig. 9d). This implies that the ideal heat-treated temperature for porous mayenite monolith is approximately 1000 ℃. Similarly to the as-dried gels, the sample heat-treated in air at 1000 ℃ exhibits narrow macropore distribution, confirmed by mercury intrusion (Fig. 9e). Pore size decreases after heat-treatment due to the shrinkage of network. However, pore volume and skeletal density (1.69 cm^3 g^{-1} and 2.32 cm^3 g^{-1} to as-dried and heat-treated samples, respectively) are obviously increased. It indicates that the shrinkage of network leads to finer and denser skeleton, but has little effect on macropores, which is consistent with the SEM results. In addition, the heat-treated sample at 1000 ℃ possesses high porosity of 72.9 %.

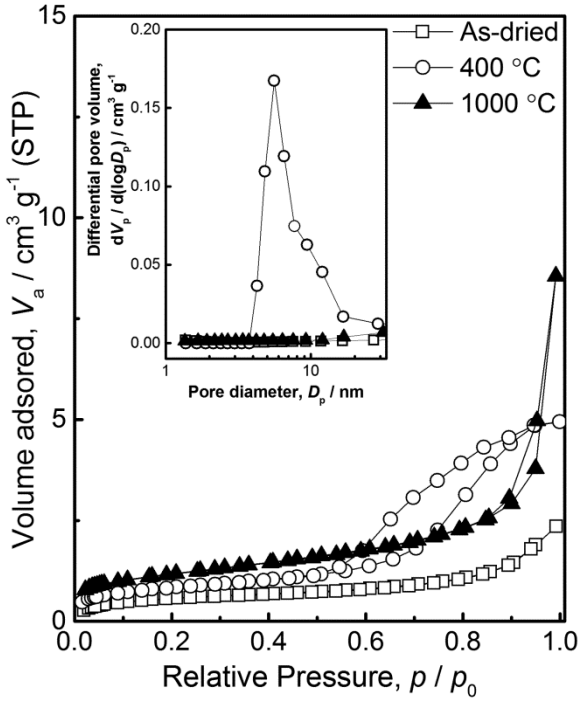

Fig. 10 Nitrogen adsorption-desorption isotherm of samples as-dried and heat-treated in air at different temperature. Inset shows the corresponding BJH pore size distribution curve.

Fig. 10 shows nitrogen adsorption-desorption isotherm of as-dried and heat-treated samples, and the corresponding BJH pore size distributions are depicted in the inset. The uptake at low relative pressure is derived from the existence of micropores. It indicates that both as-dried and heat-treated samples have few micropores. BET analysis indicates that each sample has BET surface area smaller than 5 m^2 g^{-1}, since the BET surface area mainly depends on the amount of micropores. Revealed form BJH data, some mesopores of about 5-7 nm form in the sample heat-treated at 400 ℃, whereas other ones possess almost no mesopores. Small mesoporoes in heat-treated samples originate from the interstices among primary particles,[35] and given the heat-treated samples consist of several organic species, these mesopores appear at 400 ℃ derive from the combustion of organic species in the skeleton. However, no mesopores are found in sample heat-treated at 1000 ℃ due to further densification of skeleton above crystallization temperature.

4 Conclusions

Monolithic mayenite with well-defined macropores has been successfully synthesized from ionic precursors via a facile epoxide-mediated sol-gel route accompanied by phase separation. The appropriate choice of the amount of starting solvents, poly(ethylene oxide) and propylene oxide allows the formation of the co-continuous macroporous gel. PEO is used as a phase separation inducer and is preferentially distributed into the liquid phase. Using Glycol as a chelating agent and formamide as a drying control chemical additive, homogeneous gels with no obvious shrinkage after drying are obtained. The dried gels are amorphous and transform to $Ca_{12}Al_{14}O_{32}Cl_2$ after careful heat-treatment at 1000 ℃, while the macroporous structure as well as the monolithic shape is retained. In addition, the porous monoliths before and after heat-treatment both possess high porosity as well as smooth and dense skeletons with few micro-mesopores.

It is expected that further improvements to the macroporous structure and crystalline phase will be achieved by optimization of the starting compositions in the future. Furthermore, the obtained monolithic mayenite with well-defined macropores can find various electrochemical applications through further reduction treatment (such as Ca reduction), and this well be discussed in another work.

Acknowledgements

This work is supported by the National Natural Science Foundation of China (51372225) and Zhejiang Provincial Natural Science Foundation of China (LY13B010001).

Notes and references

[a] *Department of Materials Science and Engineering, Zhejiang University, Hangzhou, 310027, China.*
[b] *Department of Chemistry, Graduate School of Science, Kyoto University, Kitashirakawa, Sakyo-ku, Kyoto 606-8502, Japan*
E-mail: yanghui@zju.edu.cn.
† Electronic Supplementary Information (ESI) available: See DOI: 10.1039/b000000x/

1 H. Bartl and T. Scheller, *Neues Jahrb. Mineral., Monatsh.*, **1970**, 35, 547.
2 J. A. Imlach, L. S. D. Glasser and F. P. Glasser, *Cem. Concr. Res.*, **1971**, 1, 57.
3 H. Hosono and Y. Abe, *Inorg. Chem.*, **1987**, 26, 1192.
4 R. W. Nurse, J. H. Welch and A. J. Majumdar, *Trans. Br. Ceram. Soc.*, **1965**, 64, 323.
5 J. Jeevaratnam, F. P. Glasser and L. S. D. Glasser, *J. Am. Ceram. Soc.*, **1964**, 47, 105.

6 J. Li, F. Huang, L. Wang, S.Q. Yu, Y. Torimoto, M. Sadakata and Q.X. Li, *Chem. Mater*., **2005**, 17, 2771.
7 K. Hayashi, M. Hirano, S. Matsuishi, H. Hosono, *J. Am. Chem. Soc*., **2002**, 124, 738.
8 K. Hayashi, S. Matsuishi, T. Kamiya, M. Hirano and H. Hosono, *Nature*, **2002**, 419, 462.
9 M. Miyakawa, K. Hayashi, M. Hirano, Y. Toda, T. Kamiya and H. Hosono, *Adv. Mater*., **2003**, 15, 1100.
10 S. Matsuishi, Y. Toda, M. Miyakawa, K. Hayashi, T. Kamiya, M. Hirano, I. Tanaka and H. Hosono, *Science*, **2003**, 301, 626.
11 Y. Toda, S. Matsuishi, K. Hayashi, K. Ueda, T. Kamiya, M. Hirano, H. Hosono, *Adv. Mater*., **2004**, 16, 685.
12 S. Matsuishi, K. Hayashi, M. Hirano and H. Hosono, *J. Am. Chem. Soc.* **2005**, 127, 12454.
14 P. V. Sushko, A. L. Shluger, K. Hayashi, M. Hirano and H. Hosono, *Phys. Rev. Lett.*, **2003**, 91, 126401.
15 Z. Li, J. Yang, J. G. Hou, Q. Zhu, *Angew. Chem., Int. Ed.*, **2004**, 43, 6479.
16 D. K. Lee, L. Kogel, S. G. Ebbinghaus, I. Valov, H. D. Wiemhoefer, M. Lerch and J. Janek, *Phys. Chem. Chem. Phys.*, **2009**, 11, 3105.
17 P. V. Sushko, A. L. Shluger, M. Hirano and H. Hosono *J. Am. Chem. Soc.*, **2007**, 129, 942.
18 Toda, Y.; Yanagi, H.; Ikenaga, E.; Kim, J. J.; Kobata, M.; Ueda, S.;Kamiya, T.; Masahiro, H.; Kobayashi, K. Hosono, H. *Adv. Mater.* **2007**, 19, 3564.
19 S. Matsuishi, T. Nomura, M. Hirano, K. Kodama, S. Shamoto and H. Hosono, *Chem. Mater*., **2009**, 21, 2589.
20 K. Ozawa, N. Sakamota, N. Wakiya, H. Suzuki, *J. Ceram. Soc. Jpn.*, **2011**, 119, 469.
21 K. Kurashige, Y. Toda, S. Matstuishi, K. Hayashi, M. Hirano and H. Hosono, *Cryst. Growth Design*, **2006**, 6, 1602.
22 M. Zahedi, A.K. Ray and D.S. Barratt, *J. Phys. D: Appl. Phys.*, **2008**, 41, 035404.
23 M. Miyakawa, M. Hirano, T. Kamiya and H. Hosono, *Appl. Phys. Lett.*, **2007**, 90, 182105.
24 K. Nakanishi and N. Tanaka, *Acc. Chem. Res.*, **2007**, 40, 863.
25 A. Kitada, G. Hasegawa, Y. Kobayashi, K. Kanamori, K. Nakanishi and H. Kageyam, *J. Am. Chem. Soc*., **2012**, 134, 10894.
26 G. Hasegawa, T. Sato, K. Kanamori, K. Nakano, T. Yajima, Y. Kobayashi, H. Kageyama, T. Abe and K. Nakanishi, *Chem. Mater*., **2013**, 25, 3504.
27 K. Nakanishi, *J. Porous Mater*., **1997**, 4, 67.
28 K. Kawamoto, K. Nakanishi and T. Hanada, *Proceedings of Symposium on Organic-Inorganic Hybrid Materials*, San Francisco, CA, Apr 09-13, **2008**, Vol. 1007, pp 63-68.
29 R. Dorin, H. Sai and U. Wiesner, *Chem. Mater*., **2014**, 26, 339.
30 A. E. Gash,; T. M. Tillotson,; J. H. Satcher, J. F. Poco, L. W. Hrubesh and R. L.Simpson, *Chem. Mater*., **2001**, 13, 999.
31 A. E. Gash, T. M. Tillotson, J. H. Satcher, L. W. Hrubesh and R. L. Simpson, *J. Non-Cryst. Solids*, **2001**, 285, 22.
32 A. E. Gash,; Satcher, J. H.; Simpson, R. L. *J. Non-Cryst. Solids* **2004**, 350, 145.
33 A. E. Gash, J. H. Satcher and R. L. Simpson, *Chem. Mater.*, **2003**, 15, 3268.
34 Y. Tokudome, K. Fujita, K. Nakanishi, K. Miura and K. Hirao, *Chem. Mater*., **2007**, 19, 3393.
35 J. Konishi, K. Fujita, S. Oiwa, K. Nakanishi and K. Hirao, *Chem. Mater*., **2008**, 20, 2165.
36 Y. Kido, K. Nakanishi, A. Miyasaka, K. Kanamori, *Chem. Mater*., **2012**, 24, 2071.
37 X. Z. Guo, H. Yu, H. Yang, K. Kanamori, Y. Zhu and K. Nakanishi, *J. Porous Mater*., 2013, 20, 1477.
38 X. Z. Guo, W. Y. Li, H. Yang, K. Kanamori, Y. Zhu and K. Nakanishi, *J Sol-Gel Sci. Technol.*, **2013**, 67, 406.
39 G. Hasegawa, Y. Ishihara, K. Kanamori, K. Miyazaki, Y.Yamada, K. Nakanishi and T. Abe, *Chem. Mater*., 2011, 23, 5208.
40 W. Y. Li, Y. Zhu, X. Z. Guo, K. Nakanishi, K. Kanamori and H. Yang, *Sci. Technol. Adv. Mater*., **2013**, 14, 045007.
41 X. Z. Guo, W. Y. Li, K. Nakanishi, K. Kanamori, Y. Zhu and H. Yang, *J. Eur. Ceram. Soc*., **2013**, 15, 3268.
42 X. Z. Guo, K. Nakanishi, K. Kanamori, Y. Zhu and H. Yang, *J. Eur. Ceram. Soc.*, **2014**, 34, 817.
43 Y. Tokudome, A. Miyasaka, K. Nakanishi and T. Hanada, *J. Sol-Gel Sci. Technol.*, **2011**, 57, 269.
44 M. L. Calzada, R. Sirera, F. Carmona and B. Jimenez, *J. Am. Ceram. Soc*., **1995**, 78, 1802.
45 W. Y. Li, X. Z. Guo, Y. Zhu, H. Yang, K. Kanamori and K. Nakanishi, *J. Sol-Gel Sci. Technol.*, **2013**, 67, 639.
46 N. Viart and J. L. Rehspringer, *J. Non-Cryst. Solids*, **1996**, 195, 223.
47 A. V. Rao, H.M. Sakhare, A.K. Tamhankar, M.L. Shinde, D.B. Gadave and P.B. Wagh, *Mater. Chem. Phys.*, **1999**, 60, 268.
48 J. Konishi, K. Fujita, K. Nakanishi and K. Hirao, *Chem. Mater.*, **2006**, 18, 6069.
49 J. Konishi, K. Fujita, K. Nakanishi and K. Hirao, *Chem. Mater.*, **2006**, 18, 864.
50 G. Hasegawa, K. Kanamori, K. Nakanishi and T. Hanada, *J. Am. Ceram. Soc*., **2010**, 93, 3110.
51 S. J. Karlik, E. Tarien, G. A. Elgavish and G. L. Eichhorn, *Inorg. Chem*., **1983**, 22, 525.
52 J. D. Kubicki, D. Sykes and S. E. Apitz, *J. Phys. Chem. A*, **1999,** 103, 903.
53 S .N. Ude, C. J. Rawn, R. A. Peascoe, M. J. Kirkham, G. L. Jones and E. A. Payzant, *Ceram. Int.*, **2014**, 40, 1117.
54 J. Q. Sun, L. Gong L, J. Shen, Z. Lin and Q.X. Li, *Acta Phys. -Chim. Sin.*, **2010**, 26, 795-798.

Graphical Abstract

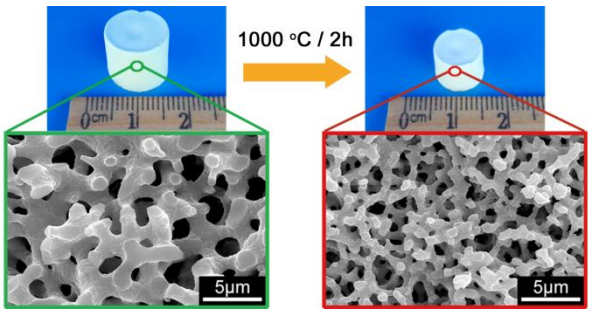

Monolithic mayenite has been successfully prepared via sol-gel process followed by heat-treatment, exhibiting co-continuous macroporous structure and high porosity.